Max-Planck-Institut
für Meteorologie

REPORT No. 31

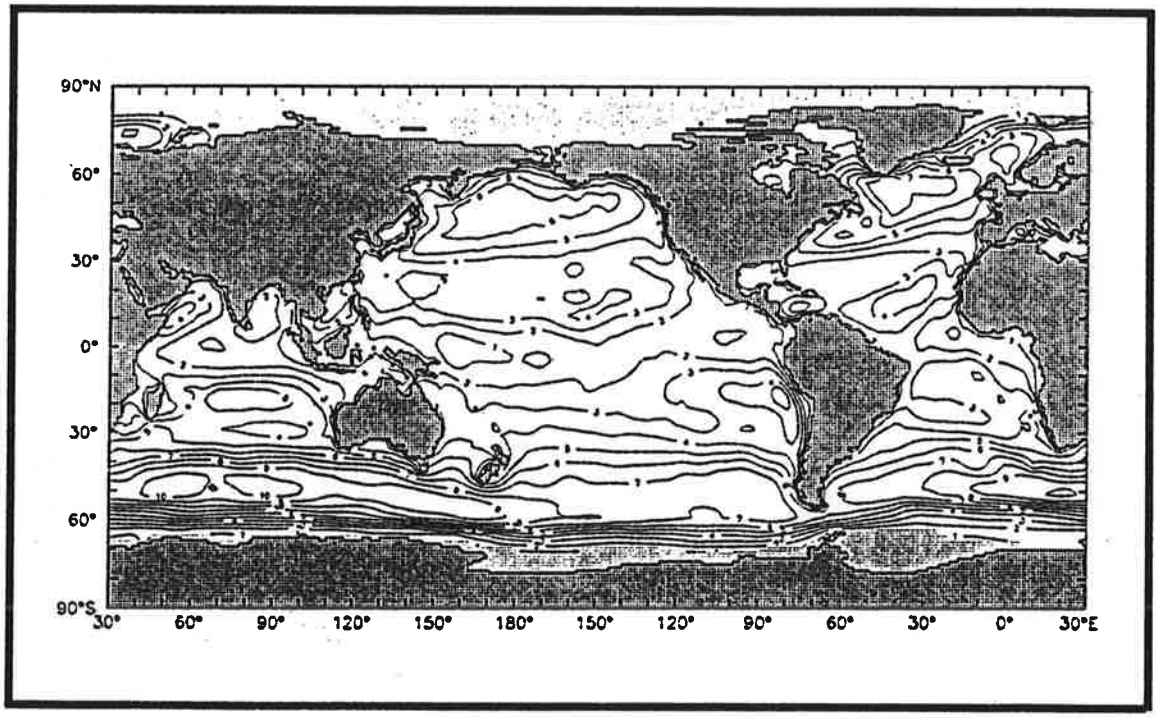

SPATIAL AND TEMPORAL VARIATION OF THE GAS EXCHANGE COEFFICIENT FOR CO_2: 1. DATA ANALYSIS AND GLOBAL VALIDATION

by

MARTIN HEIMANN • PATRICK MONFRAY

HAMBURG, MAY 1989

AUTHORS:

MARTIN HEIMANN

MAX-PLANCK-INSTITUT
FUER METEOROLOGIE

PATRICK MONFRAY

MAX-PLANCK-INSTITUT
FUER METEOROLOGIE

CENTRE DES FAIBLES RADIOACTIVITÉS
CNRS
F-91198 GIF-SUR-YVETTE CEDEX
FRANCE

MAX-PLANCK-INSTITUT
FUER METEOROLOGIE
BUNDESSTRASSE 55
D-2000 HAMBURG 13
F.R. GERMANY

Tel.: (040) 4 11 73-0
Telex: 211092
Telemail: MPI.Meteorology
Telefax: (040) 4 11 73-298

Spatial and Temporal Variation of the Gas Exchange Coefficient for CO_2: 1. Data Analysis and Global Validation

Martin Heimann Patrick Monfray*

Max-Planck-Institut für Meteorologie
Bundesstrasse 55
D-2000 Hamburg 13 (FRG)

Abstract

Based on archived ship reports (Comprehensive Ocean-Atmosphere Data Set) and meteorological analyses from the European Center for Medium-Range Weather Forcast we have constructed a climatology of surface windspeed over the ocean consisting of monthly means and standard deviation on a global 2° by 2° horizontal resolution grid. Representing the local instantaneous windspeed by means of a Weibull frequency distribution, where the parameters are determined from the monthly mean value and standard deviation, we evaluated the global spatial and temporal distribution of the gas exchange coefficient for CO_2 based on the recently proposed parametrization by Liss and Merlivat [1986]. Climatological sea surface temperatures have been used in the specification of the Schmitt number. The effects of sea ice, which is assumed to inhibit gas exchange, is also taken into account. The resulting globally and annually averaged value of the exchange coefficient, 0.0356 mol m^{-2} yr^{-1} μatm^{-1}, is a factor of 1.7 smaller than previous estimates based on either the natural radiocarbon balance between the air and the sea or the oceanic uptake of excess bomb radiocarbon as measured during the GEOSECS expeditions. The fields of the exchange coefficient exhibit large contrasts between high and low latitudes (a factor of 4) which can be validated in principle by means of the preindustrial assumed steady state air-sea distribution of the carbon isotope ratio $^{13}C/^{12}C$.

1 Introduction

The exchange of carbon dioxide between the air and the sea constitutes a key process which has to be adressed in modelling the global cycling of carbon and its isotopes. Classically, this exchange flux is represented by means of a bulk formula, i.e. by a bulk coefficient for gas exchange multiplied by the difference in partial pressure of CO_2 in the the air and water phase, in analogy to the standard bulk formulas used for describing momentum and energy transfer between the air and the sea. In early carbon cycle models the numerical value assigned to the bulk coefficient usually has been derived from a consideration of the global natural radiocarbon balance between the air and the sea or from observations of the oceanic uptake of bomb-produced radiocarbon [Bolin et al., 1982, Broecker et al., 1985, Broecker et al., 1986]. Such indirect methods provide only an estimate of the global average of the bulk coefficient, which was sufficient for all practical purposes at that time. The introduction of a new generation of carbon cycle models, resolving the major carbon compartments in two or three spatial dimensions [e.g. Pearman et al., 1986, Maier-Reimer and Hasselmann, 1987], however, requires a more detailed assessment of gas exchange

*also at: Centre des Faibles Radioactivités, CNRS, F-91198 Gif-sur-Yvette CEDEX (France)

fluxes on temporal scales of a few weeks and on spatial scales of a few degrees latitude and longitude.

The exchange flux of low to moderately soluble gases, such as CO_2, between the atmosphere and the surface waters of the ocean is controlled by a thin ($\sim$100 μm) boundary layer on the water side of the interface, within which molecular diffusion exceeds transport by turbulent motions [Jähne et al., 1987]. The state of this boundary layer (as given e.g. by its temperature and thickness, the latter being itself a function of the local structure of micro turbulence) determines the gas transfer, given a driving partial pressure difference between the adjacent bulk air and sea phase. In the presence of breaking waves it is believed that entrained bubbles contribute to the gas flux [Merlivat and Memery, 1983]. Several microphysical models of this boundary layer have been constructed (see e.g. Coantic [1986] or Back and McCready [1988]), but, unfortunately, up to now these models do not permit a quantitative determination of the bulk coefficient given a set of readily observable environmental parameters, such as surface windspeed and sea surface temperature.

Alternatively, using an empirical approach, the bulk coefficient may be specified as a simple function of windspeed and sea surface temperature which is fitted to measurements. However, direct observations of CO_2 gas exchange fluxes under natural conditions suffer from several limitations as discussed in detail by Broecker et al. [1986]. Likewise, the results of laboratory studies on wind/wave tunnels show considerable scatter and are not easily extrapolated to large scale natural environments. Therefore, the most promising empirical approach to determine the bulk coefficient for gas exchange has been by means of other trace gases, most notably the radioactive noble gas ^{222}Rn [Peng et al., 1979, Roether and Kromer, 1984, Smethie et al., 1985], the results of which can be translated to the CO_2 gas by means of an assumed dependency on the molecular diffusivity.

Recently, Liss and Merlivat [1986] proposed an empirical quantitative relationship between bulk coefficient and windspeed at 10m height, which was derived from the data of an experiment reported by Wanninkhof et al. [1985], who monitored the escapement of a purposefully injected trace gas (SF_6) from a lake. Subsequently this formulation has been used by several investigators in order to evaluate the bulk coefficient on a global scale using various sources of windspeed data, such as archived ship reports [Eriksson and Duce, 1987], meteorological analyses [Thomas et al., 1988] or measurements from satellite based scatterometer data [Etcheto and Merlivat, 1989]. All of these studies are limited in that they cannot provide global ocean coverage [Eriksson and Duce, 1987] or climatological representativity [Thomas et al., 1988, Etcheto and Merlivat, 1989].

In the present paper we describe the results of a study using a similar approach. Firstly we critically evaluate the available data on windspeed from archived ship observations and from meteorological analyses. By forming a composite from both sources of data we present an attempt to establish a monthly climatology of surface windspeed data on a global 2° by 2° grid. In addition we obtain a measure of the distribution of the instantaneous wind around the monthly mean at each grid location. From meteorological analyses covering the period 1981 through 1986 we also estimate a measure of the interannual variability of the surface windspeed. By means of the parametrization of Liss and Merlivat [1986] in conjunction with sea surface temperature and ice cover data we subsequently compute a global monthly climatology of the bulk coefficient for gas exchange for CO_2. Finally, we present an attempt to validate the resulting coefficient fields by means of observations of the carbon isotopes ^{13}C and ^{14}C.

In a sequel to the present paper [Monfray et al., 1989] we explore the consequences of a temporally and spatially varying bulk coefficient for gas exchange with respect to the modelling of the oceanic uptake of bomb produced radiocarbon and of anthropogenic CO_2.

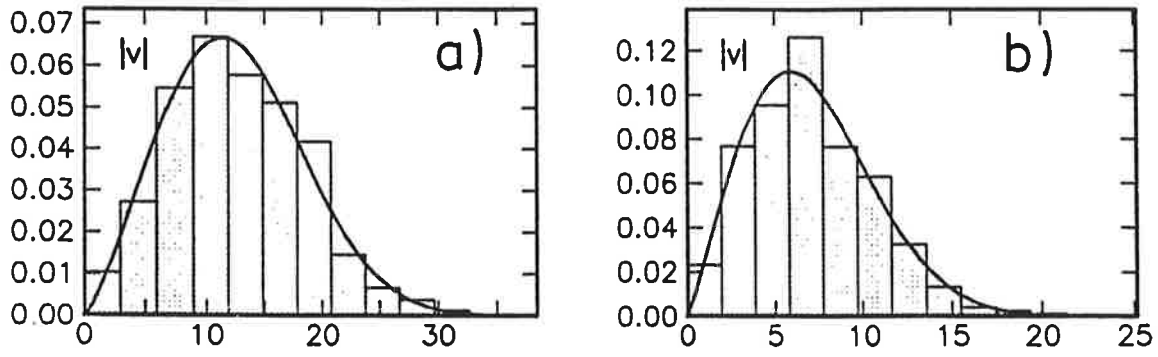

Figure 1: Frequency histogram of instantaneous windspeed at weathership D positioned in the North Atlantic (44°N, 41°W) for (a) January and (b) July. The solid curve represents the continuous Weibull distribution fitted to the data (see text).

2 Assessment of Surface Wind Data

The present analysis of surface wind speed was based on two primary data sources:

1. Climatological data of monthly mean windspeed and standard deviation from ship observations as compiled in the Comprehensive Ocean-Atmosphere Data Set (COADS).
2. Daily meteorological analyses from the European Center for Medium Range Weather Forecast (ECMWF) for the period 1981 through 1986.

In addition we also investigated records of high quality windspeed data from specific locations, such as from:

- eight weatherships located in the North Atlantic,
- the German R.V. Meteor while stationed in the tropical Atlantic in the summer of 1979,
- buoys located in the tropical Atlantic and Pacific oceans.

These records allow us to assess the statistics of the surface windspeed over the ocean, but they also provide a means to validate the primary data sets at a few specific points.
This section describes the processing of each data set and the procedures employed to establish a global climatology of surface windspeeds.

2.1 The Frequency Distribution of the Surface Windspeed

In a first step we examined the weathership data in order to find a suitable statistical description of the instantaneous windspeed. The Deutscher Wetterdienst (DWD) kindly provided us with the records from eight weatherships located in the North Atlantic. These data consisted of 3-hourly reports of the 10 m windspeed and direction, covering a time period of almost 25 years. For each weathership and each month of the year all reports from the entire data set were merged and displayed as histograms. As an example Figure 1 displays the histograms for January and July at Weathership D (44°N, 41°W), based on 20 years of 3-hourly data. Similar histograms were obtained at all locations and for each month of the year. We found that the frequency

distribution, $f(v)$, of the instantaneous windspeed, v, may satisfactorily be represented by means of a Weibull distribution, analogous to the surface windspeed over land [Justus et al., 1977, Stewart and Essenwanger, 1978]:

$$f(v) = \frac{a}{c} e^{-(\frac{v}{c})^a} (\frac{v}{c})^{a-1} \tag{1}$$

Given mean windspeed $\overline{v}$ and standard deviation σ_v, the two parameters of the distribution, a and c, may be estimated from:

$$a \approx (\frac{\sigma_v}{\overline{v}})^{-1.086} \tag{2}$$

and

$$c = \frac{\overline{v}}{\Gamma(\frac{1}{a}+1)} \tag{3}$$

As an example we display in Figure 1 the fitted Weibull frequency distributions (solid lines). Thus, the assessment of the statistics of surface windspeed is reduced to the task of determining monthly mean and standard deviation.

2.2 Archived Ship Observations

In a second step climatological monthly means and standard deviation of the 10 m windspeed were derived from the Comprehensive Ocean-Atmosphere Dataset [COADS Release 1, Woodruff et al., 1987]. This dataset is compiled from over $7 \cdot 10^7$ archived and quality checked ship observations of meteorological and oceanographic variables. At our disposal was the "trimmed monthly summaries" product from the COADS data set, containing, among other variables, for each box of a global 2° by 2° latitude-longitude grid and each month since 1860 an estimate of mean and standard deviation of 10 m windspeed together with the number of ship observations. For each grid box we examined all January records from the time period 1950–1979 and selected only records with more than six ship observations. From these selected years we calculated the climatological January mean. Thereby each individual January record was weighted according to the corresponding number of observations. Also, we obtained an estimate of the standard deviation of individual observations around the mean, which was calculated from the square root of the weighted mean of the squared individual standard deviations of the selected January records. In addition in each grid box we calculated the sum of all observations from the selected January records.
This same procedure was subsequently performed for each of the remaining months of the year. By this procedure we obtained 12 monthly maps of mean windspeed, standard deviation of windspeed and number of constituting ship observations.
The established climatology based on the COADS data set, however, suffers from several drawbacks. Many regions of the World Ocean are only sparsely sampled, thus leading to climatological values lacking representativity. More seriously, there exist vast regions, mostly in the winter season in the southern oceans, which are not covered at all. An impression of the density of data coverage may be obtained from the maps displayed in Figures 4 and 5 where the shaded oceanic regions indicate grid cells with more than 200 observations. Because of these deficiencies, we are not able to evaluate the coefficient for gas exchange on a global scale from these data.

2.3 Meteorological Analyses of Surface Windspeed

Lastly, we investigated wind data from the archived meteorological analyses of the ECMWF. These analyses are routinely produced by the Center's global four-dimensional data assimilation system, which blends, in a consistent way, individual meteorological observations with the previous 6 hour forcast from the operational global weather model [Bengtsson et al., 1982, Lorenc, 1981].

Daily fields of the u- and v- wind components on the 1000 hPa analysis surface were made available to us through the Deutsche Wetterdienst (DWD) for the entire time period 1979–1986. The fields at our disposal had the same spectral resolution as the T42 version of the European Center's forecast model (in the original assimilation scheme at ECMWF a higher spatial resolution is used). The approximate horizontal resolution of the fields in physical space is 2.8125° latitude and longitude. For the present study all fields were interpolated horizontally using two-dimensional Hermite cubics [de Boor, 1978] onto the 2° by 2° grid of the COADS dataset.

At first we investigated the relationship between these analyses nominally ascribed to the 1000 hPa surface and the windspeed at 10 m height above the sea surface. According to the documentation of the European Center's assimilation system for any given analysis time instant at most grid locations the analyzed value of the wind components as recorded on the 1000 hPa surface is obtained from the previous 6 hour model forecast. Since the ECMWF forecast model uses a reduced pressure vertical coordinate system in the lowest layers, vertical interpolation is used to obtain the value on the 1000 hPa surface, or, whenever this surface lies below the lowest model layer the values of the u- and v- components on the lowest model layer are directly ascribed to the 1000 hPa surface. The lowest layer of the forecast model is located at a height of $0.9961 p_s$, where p_s denotes the surface pressure. This corresponds to a height of typically 30 m above the Earth's surface. Thus, the values recorded on the 1000 hPa analysis surface represent a height above surface of 30 m or more. An unambiguous extrapolation of the 1000 hPa windspeeds to the height of 10 m as required for our purpose is not possible without a detailed reconstruction of the boundary layer at every grid point and time instant; an excercise which we did not attempt to do. Based on this consideration we would expect the 1000 hPa windspeeds in general to overestimate the 10 m wind. The magnitude of this possible overestimation could be on the order of 20%: e.g. under neutral conditions the 10 m windspeed is 11% smaller than the 30 m windspeed and about 20% smaller than the windspeed at 100 m height (assuming a roughness length of 10^{-3}m).

As an alternative to an elaborate boundary layer computation, we compared pointwise the daily analyses with available ship and buoy data. To this end we used daily 10 m windspeed reports from four weatherships in the North Atlantic which were still in operation after 1978, supplemented by data from the German R.V. Meteor in the tropical Atlantic ocean in the summer of 1979. Furthermore, we obtained data from a buoy located in the Gulf of Guinea (4°W, 0°N) from the years 1983 and 1984 [C. Colin and J. Boutin, personal communication, Colin and Garzoli, 1987] and, finally, we were able to examine windspeed data from 4 buoys located on the equator in the Pacific ocean [McPhaden, personal communication, 1988]. The Pacific ocean buoy data were recorded at an anemometer height of 3.8 m; they were subsequently multiplied by a factor of 1.1 to obtain an estimate of the 10 m windspeed. A similar correction was applied to the Golf of Guinea buoy data.

By horizontal linear interpolation we obtained the daily windspeed from the EC analyses at the locations of the weatherships and the buoys. These values were then correlated to the observed windspeeds at the same time instant.

The result of the comparison is summarized in Table 1, where we list for each site mean windspeed and average standard deviation obtained from both sources of data together with the root mean square difference between observations and interpolated value from the analyses. The calculation of the means and the standard deviations is based only on time records for which observations and analyses were available. In the case of the buoy data from the Golf of Guinea the comparison is based only on monthly means.

The agreement between the two sources of data is remarkably good, especially at the North Atlantic weatherships. Indeed, here no systematic deviation is discernible, neither between the mean values nor between the standard deviations.

Table 1: Comparison of Windspeeds from Meteorological Analyses and Direct Observations

Location	Time Period	Mean [ms^{-1}]		Standard Deviation [ms^{-1}]		RMS-Difference [ms^{-1}]
		Obs.	Anal.	Obs.	Anal.	
Atlantic Ocean:						
OWS 1, (52.7°N, 35.5°W)	Jan.–Nov. 1979	9.93	9.97	4.58	4.51	2.38
OWS 2, (57.2°N, 19.8°W)	Jan.–Nov. 1979	11.22	10.67	5.10	4.57	2.28
OWS 3, (66.4°N, 2.3°E)	Jan.–Nov. 1979	9.61	8.10	4.13	3.90	3.06
OWS 4, (46.8°N, 17.3°W)	Jan.–Nov. 1979	9.01	9.08	3.83	3.80	2.04
RV. Meteor, 0°N, 22°W	Feb.–Jun. 1979	5.55	4.10	2.23	1.70	2.50
Gulf of Guinea, 0°N, 4°W	Jun.–Dec. 1983	5.6	5.9	-	-	-
Pacific Ocean:						
Buoy 1, (0°N, 95°W)	Sep. 1981 – Apr. 1983	5.27	4.14	1.48	1.44	1.77
Buoy 2, (0°N, 110°W)	Mar. 1980 – Dec. 1986	5.28	4.65	1.48	1.44	1.61
Buoy 3, (0°N, 124°W)	Oct. 1983 – Oct. 1985	5.12	5.50	1.38	1.53	1.50
Buoy 4, (0°N, 140°W)	Apr. 1984 – Dec. 1986	7.01	5.47	1.41	1.32	1.89

At the tropical locations, the differences between analyses and observations are larger. The means systematically differ by 26% in the case of the R.V. Meteor data from 1979 and by 22% at Buoy 1 and at Buoy 4. In general the 1000 hPa analyses appear to underestimate the observed mean 10 m windspeed, at most by 25%. Except for the R.V. Meteor data the agreement between the standard deviations calculated from the analyses and from the observations is excellent. At all location the rms-difference between the two sources of data is smaller than 30% of the mean windspeed.

Based on the results of this comparison we adopted in this study the working hypothesis that the 1000 hPa wind from the European Center's assimilation system over the ocean may be used directly as an estimate of the 10 m surface windspeed. The possible overestimation as inferred above from the documentation of the data assimilation system in use at ECMWF is not readily seen in our comparison. Most likely it is compensated for by the spatial and temporal smoothing which inevitably occurs in the assimilation system. Nevertheless, we must be aware of a possible systematic bias when using the analyzed 1000 hPa wind as estimate of the 10 m surface windspeed.

By comparing the zonally averaged windspeeds for each of the years of the analyses to the climatology compiled from the COADS data set we noticed that the analyses for the years 1979 and 1980 in general exhibited smaller monthly mean windspeeds in the tropical belt between 20°S and 20°N. Indeed, we observed a distinct offset in the windspeed data at the beginning of 1981, when the weather model became operational at the European Center. Based on this experience we discarded the meteorological analyses of 1979 and 1980 and computed for every month of the year mean value and standard deviation from only the 6 years 1981–1986. In addition, we also determined for each month of the year the standard deviation from the 6 years as an indicator of the interannual variability of the monthly mean windspeed.

2.4 Construction of Composite Climatology

Figure 2 compares, as a function of latitude, the zonally averaged windspeed based on the two primary data sources for the months of January and July. In case of the ship data (dashed line), we selected only grid cells with more than 200 observations to form a zonal average. Due to the sparsity of cells which satisfy this criterion, data south of 40°S might not reflect the true zonal

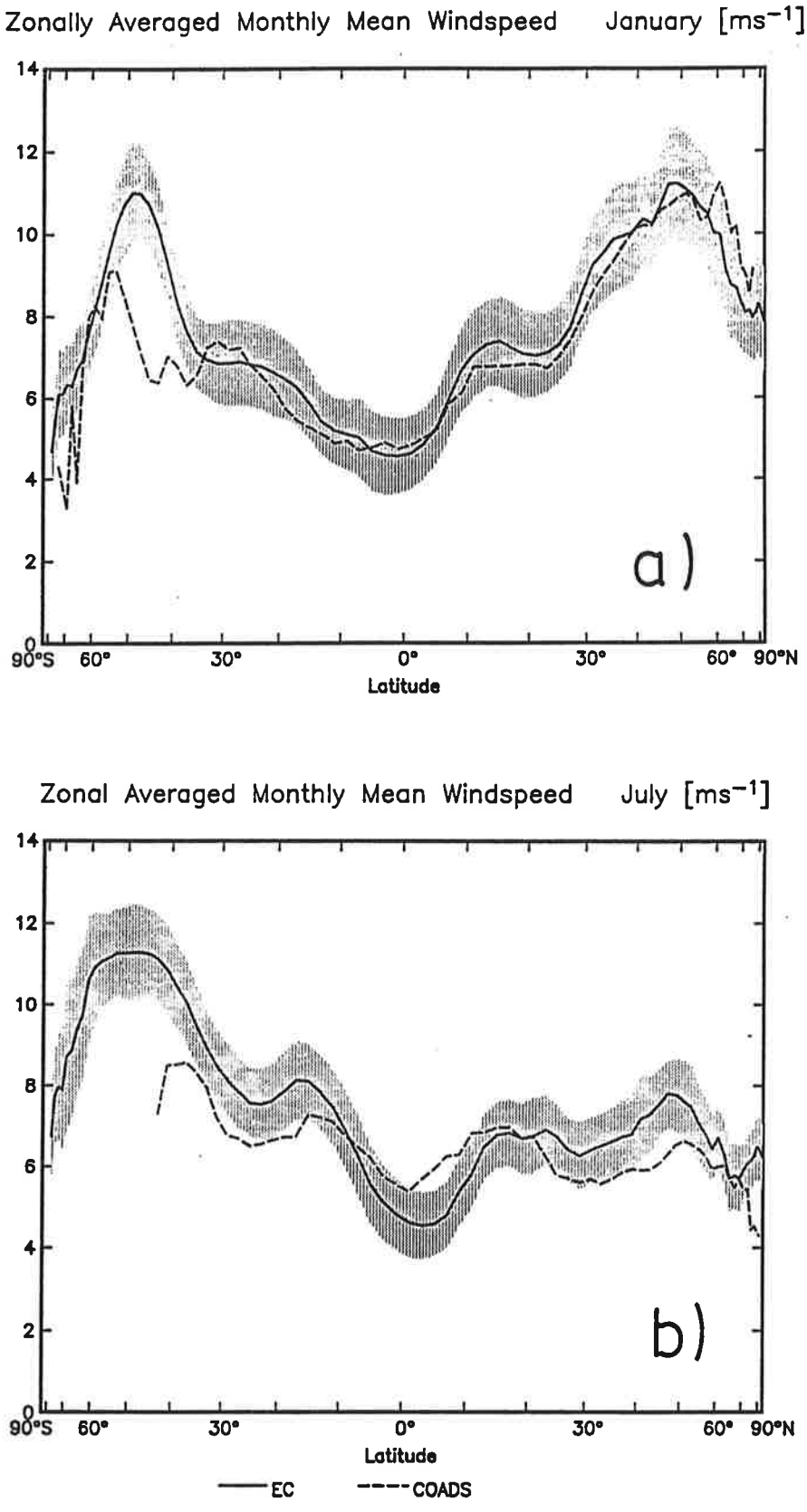

Figure 2: Zonally averaged monthly mean windspeed in ms^{-1} for (a) January and (b) July. Dashed line: estimate based on ship data; solid line: estimate based on meteorological analyses from the years 1981–1986. The shaded region around the solid line indicates ± 1 standard deviation of the individual monthly means around the 6-year mean.

average. The solid line shows the zonal mean windspeed based on the meteorological analyses. The shaded area indicates the region of ± one standard deviation of the interannual variation of the monthly means. It is seen that ship data and analyses agree very well in January north of 40°S. On the other hand, in July the ship data are consistently smaller than the analyses outside of the tropical belt, whereas within the tropical region the reverse is true.
Figure 3 compares the zonal average of the standard deviation estimated form the two sources of data. The agreement between the two independent data sets is surprising.
The comparison between the two data sets may be summarized as follows: The global annual mean windspeed, calculated from all boxes with more than 200 ship observations results in 6.99 ms^{-1} as compared to 7.47 ms^{-1} obtained from the meteorological analyses. The root mean square difference between the two data sets is 1.14 ms^{-1}. Similarly, in the case of the standard deviations the global annual mean results in 3.18 ms^{-1} based on the ship data and 3.25 ms^{-1} based on the analyses.
Because of the possible bias in the 10 m windspeed estimate based on the meteorological analyses as discussed in the previous section we believe the ship data, given a sufficient number of observations, to provide a more reliable estimate of the true climatology. Therefore, in order to produce the best estimate possible, we established a composite from the ship data and from the meteorological analyses of monthly mean windspeed and standard deviation. To this end, we selected at all locations on the 2° by 2° grid the ship value if it was based on more than 200 observations. In all other cases we choose the value from the meteorological analyses. Based on this criterion the ship value was selected on 35% of the global ocean surface.
Finally, we applied twice a 5-point smoothing operator with weight $\frac{1}{2}$ at the center and $\frac{1}{8}$ in each of the adjacent 4 grid points in order to suppress noise on length scales smaller than 4° latitude and longitude.
The resulting composite mean windspeed is shown in Figure 4 for the months of January and July. Light shading indicates regions where the ship value was selected. The composite displays a few spatial structures which may be traced back to the merging of data from the two independent data sets, as e.g. in the Atlantic ocean around 15°N in January.
The corresponding maps of the standard deviation are displayed in Figure 5. Tables 2 and 3 display zonally and annually averaged mean windspeed and standard deviation over 10° latitude bands for the three individual oceans and for the global sea surface. These data may be used to approximate the statistics of the windspeed distribution in a particular latitude band by means of equations (1)–(3). By forming the combined frequency distribution from all analysis grid boxes and all months of the year we obtain a global windspeed distribution resembling very much the Weibull-type (1), it is defined by a global, annually averaged mean windspeed of 7.38 ms^{-1} and a standard deviation of 3.89 ms^{-1}.

3 Evaluation of the Coefficient for Gas Exchange

Formally, the net gas flux from the air to the sea, F_{ex}, may be represented by means of a bulk formula:

$$F_{ex} = w(\alpha_s P_a - C_m) = w\alpha_s(P_a - P_m) \tag{4}$$

where P_a denotes the partial pressure of the gas in the atmosphere and C_m its concentration in the surface water. P_m represents the atmospheric equilibrium partial pressure of the gas corresponding to C_m, and α_s its solubility. The factor w is termed "transfer velocity" or "piston velocity" [see e.g. Broecker and Peng, 1982] and the product $w\alpha_s$ denotes the bulk coefficient for gas exchange ("gas exchange coefficient"), k_{ex}, which is customarily expressed in units of mol m^{-2} yr^{-1} μatm^{-1}.
The relationship between w and 10 m windspeed proposed by Liss and Merlivat [1986] for a gas with a constant Schmitt number (see below) of 600 was reexpressed as follows to include the

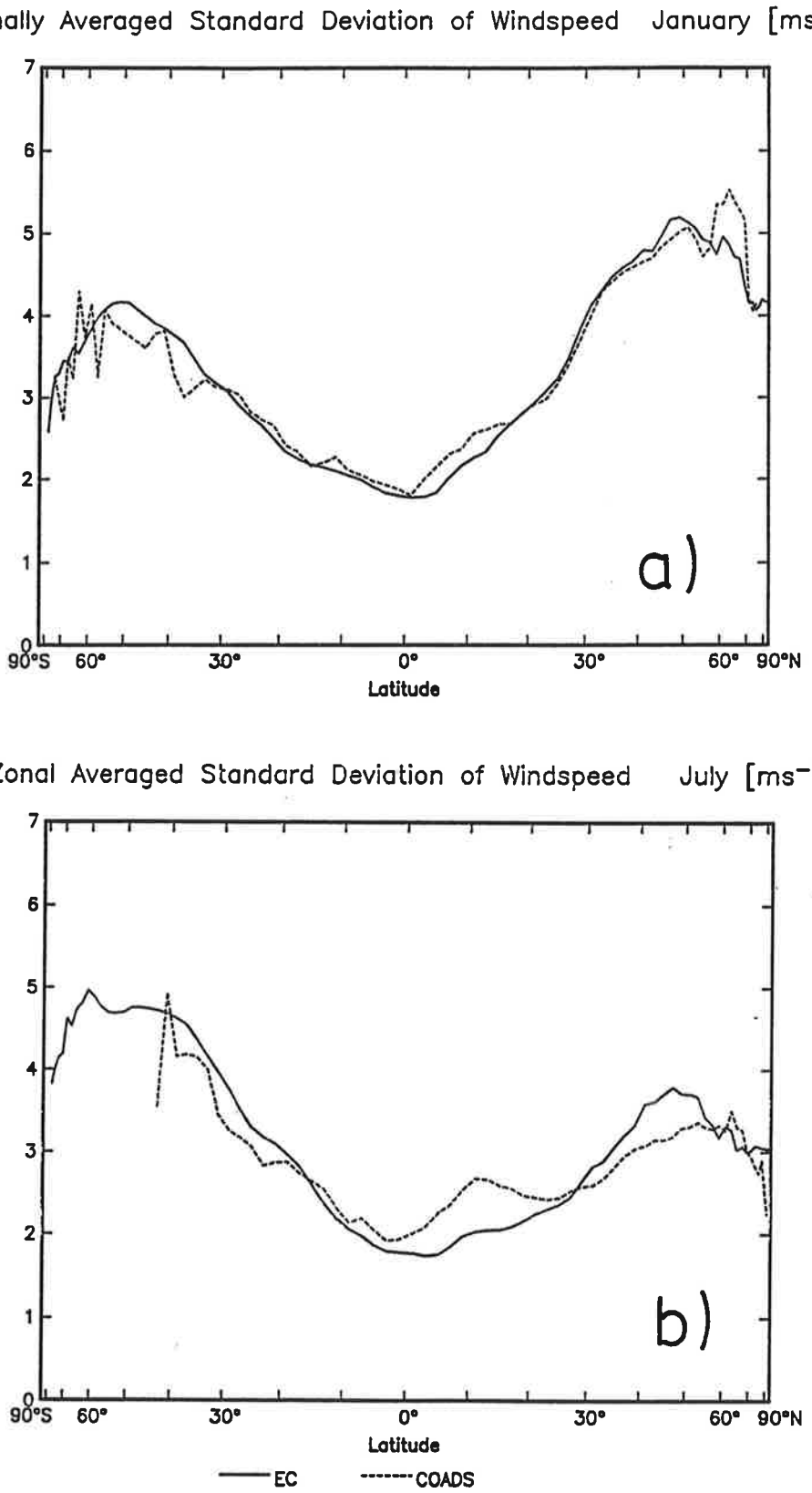

Figure 3: Zonally averaged standard deviation in ms^{-1} of the instantaneous windspeed around the monthly mean for (a) January and (b) July. Dashed line: estimate based on ship data; solid line: estimate based on meteorological analyses from the years 1981–1986.

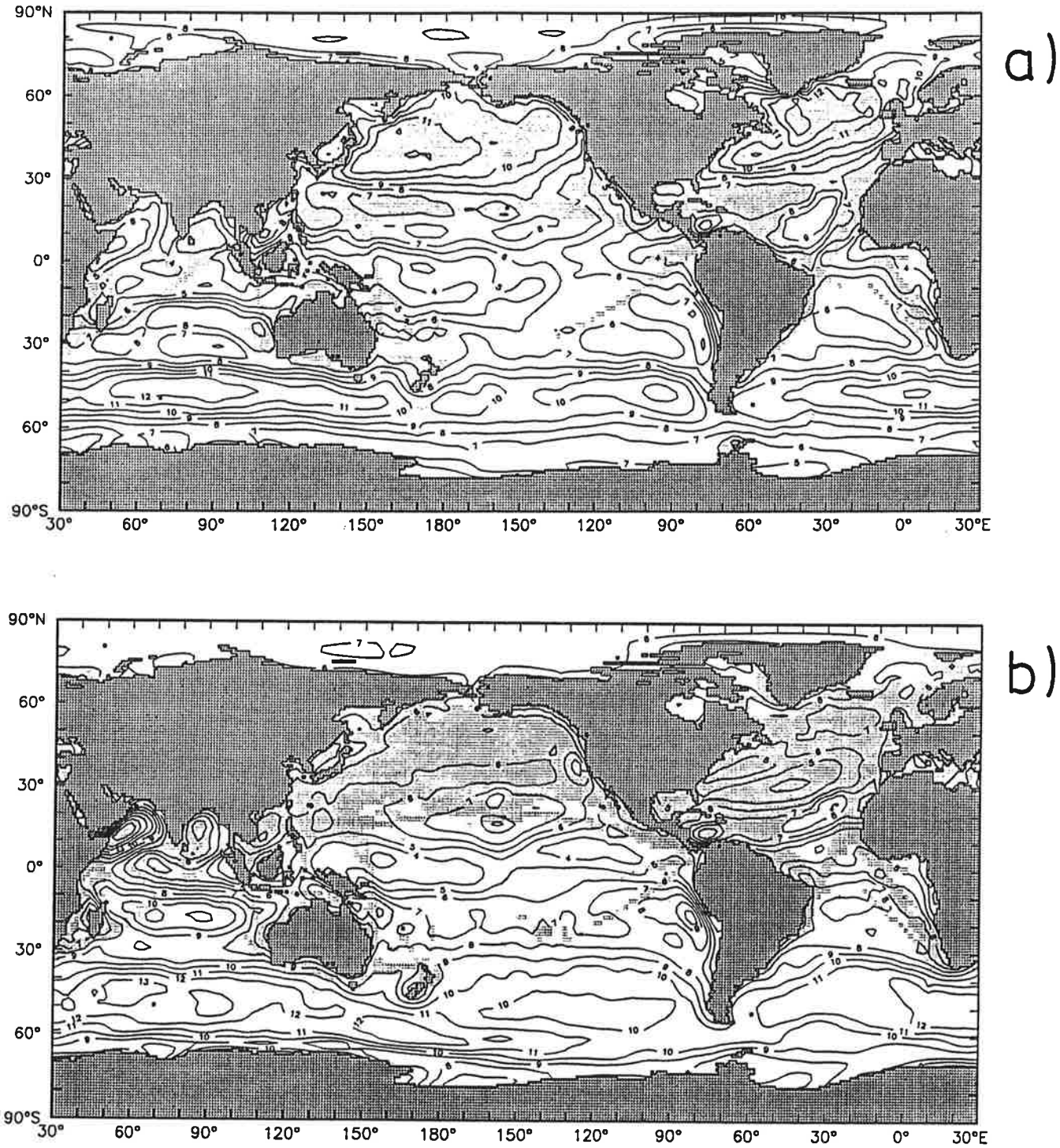

Figure 4: Monthly mean windspeed composite for (a) January and (b) July. Light shading indicates areas where the ship based values have been selected in forming the composite. The contour interval is 1 ms^{-1}.

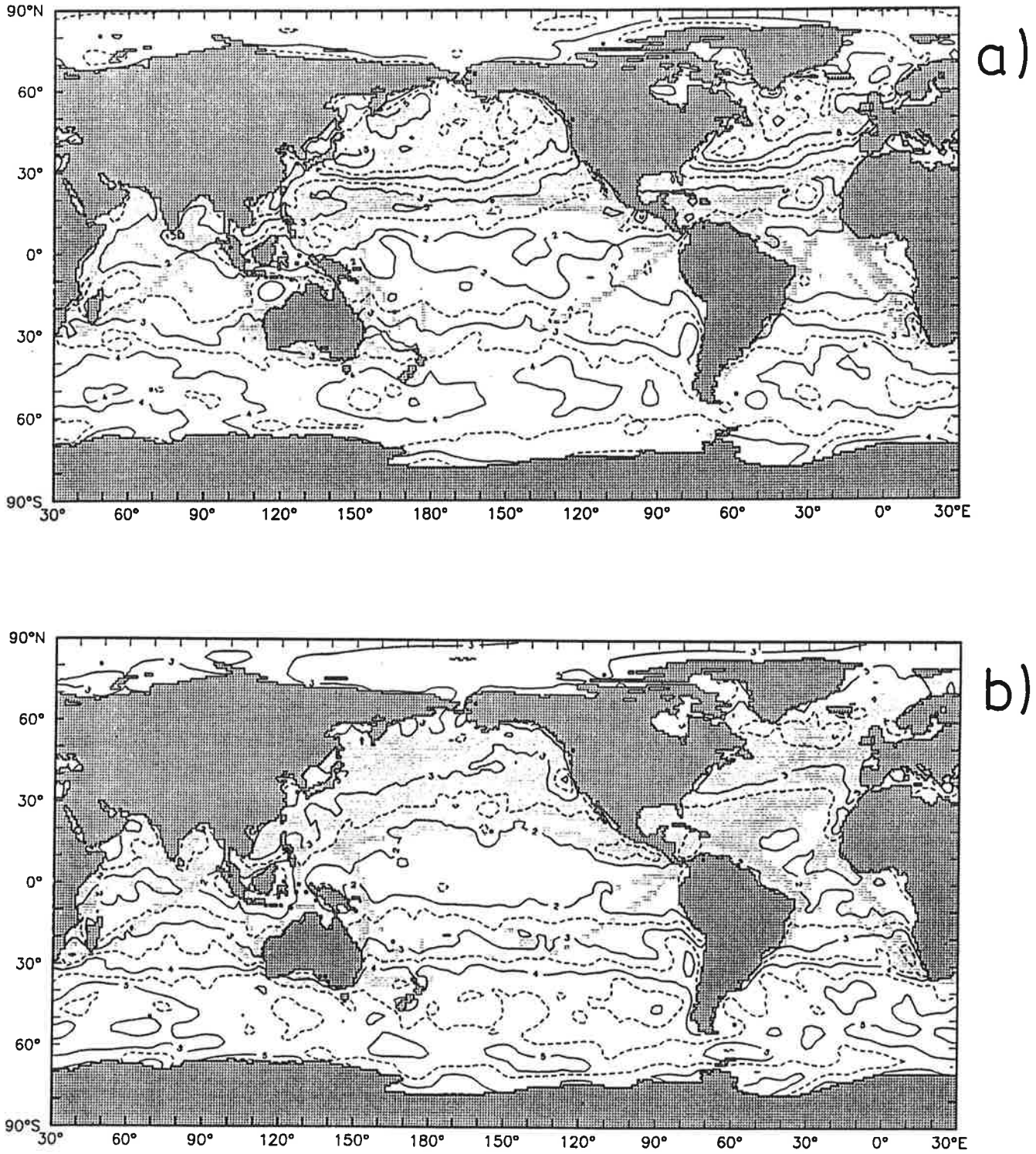

Figure 5: Composite of standard deviation of instantaneous windspeed around the monthly mean for (a) January and (b) July. Light shading indicates areas where the ship based values have been selected in forming the composite. The contour interval between solid lines is 1 ms^{-1}.

Table 2: Zonal Annual Mean Surface Windspeed [ms^{-1}]

Latitude	Atlantic	Pacific	Indian	Global Ocean
85°N	7.11			7.11
75°N	7.30			7.22
65°N	8.01	7.85		7.81
55°N	9.27	8.33		8.62
45°N	8.31	8.75		8.45
35°N	6.96	7.84		7.39
25°N	6.22	6.86	5.25	6.53
15°N	7.08	6.64	5.91	6.58
5°N	5.30	4.84	5.27	4.96
5°S	6.06	4.78	4.87	4.99
15°S	6.88	6.45	7.05	6.70
25°S	6.88	6.95	7.74	7.14
35°S	8.64	7.96	8.73	8.36
45°S	10.74	9.86	11.74	10.75
55°S	10.29	10.80	11.38	10.87
65°S	8.07	9.14	8.20	8.59
75°S	6.53	7.42		7.15

Table 3: Zonal Annual Mean Standard Deviation of Surface Windspeed [ms^{-1}]

Latitude	Atlantic	Pacific	Indian	Global Ocean
85°N	3.61			3.61
75°N	3.74			3.72
65°N	4.20	3.94		4.09
55°N	4.48	4.09		4.23
45°N	4.23	4.03		4.07
35°N	3.54	3.63		3.58
25°N	2.76	2.90	2.52	2.83
15°N	2.36	2.45	2.33	2.41
5°N	1.85	1.93	2.15	1.94
5°S	1.78	1.86	2.04	1.88
15°S	2.18	2.38	2.45	2.36
25°S	3.04	2.99	3.17	3.05
35°S	4.06	3.69	3.99	3.87
45°S	4.43	4.19	4.49	4.36
55°S	4.50	4.37	4.59	4.48
65°S	4.14	4.35	4.31	4.28
75°S	3.73	3.76		3.75

effects of temperature:

$$w(v_{10},T) = \begin{cases} 0.47\,[a(T)]^{-\frac{2}{3}} v_{10} \\ +7.44\,[a(T)]^{-\frac{1}{2}}(v_{10}-3.6)\,\mathrm{U}(v_{10}-3.6) \\ +8.47\,[a(T)]^{-\frac{1}{2}}(v_{10}-13.0)\,\mathrm{U}(v_{10}-13.0) \end{cases} \tag{5}$$

where the piston velocity, w, is expressed in 10^{-6} ms^{-1}, and the surface windspeed at 10 m height, v_{10}, is expressed in ms^{-1}. U(x) denotes the unit step function, which is 1 for $x > 0$ and 0 otherwise. The first term on the right of equation (5) reflects the dependency of the piston velocity as a function of windspeed for smooth surface conditions. The second and third term, respectively, express the enhancement of the transfer due to the presence of capillary waves at windspeeds greater than 3.6 ms^{-1} and to bubbles created by breaking waves at windspeeds above 13ms^{-1}.
The term $a(T)$ expresses the temperature dependency. It is given by

$$a(T) = \frac{Sc(T)}{600} = \frac{\nu(T)}{D(T)} 600^{-1} \tag{6}$$

where the Schmitt number, Sc, is defined as the ratio between the viscosity of water, ν, and the coefficient of molecular diffusion of the gas, D, both quantities being known functions of temperature, T. The numerical values of the exponent of $a(T)$ were chosen in accordance with the work of Jähne et al. [1987].
Equation (5) subsequently will be referred to as the LM-parametrization. It is displayed in Figure 6 as a function of windspeed for a gas with a Schmitt number of 600 (e.g. CO_2 at $T = 20$°C), together with piston velocity data obtained by the Radon method normalized to a Schmitt number of 600 (Redrawn from Liss and Merlivat [1986]; the data were compiled by Roether [1986]).
If the instantaneous windspeed is given in the form of a frequency distribution, the mean piston velocity, $\overline{w}$, is obtained from:

$$\overline{w} = \int_0^\infty f(v) w(v) dv \tag{7}$$

For each month of the year we evaluated (7) at every grid point, thereby specifying $f(v)$ as a Weibull distribution (equation (1)) where the parameters were determined from the monthly means and standard deviations as explained in the previous section. In doing so we assumed a constant sea surface temperature during each month which was obtained from the climatology constructed by Levitus [1982]. The temperature dependency of the Schmitt number was specified as listed in Appendix B. Since $w(v)$ is a piecewise linear function (see equation (5)) the integral (7) can be solved exactly in terms of incomplete gamma functions (see Appendix A). The monthly mean exchange coefficient, $\overline{k_{ex}}$, was then obtained through multiplication by α_s which was specified according to Weiss [1974] as a function of temperature (see Appendix B), thereby using a constant uniform salinity of 35‰.
Finally, the effect of ice cover in high latitude areas was incorporated by specification of the climatology of monthly mean fraction of ice cover determined by Alexander and Mobley [1976]. Ice covered sea surface was assumed to be impermeable to gas transfer, hence the coefficient fields as derived above were reduced by multiplication with the local fraction of ice-free water surface.
Figure 7 displays the resulting fields for the months of January and July, respectively. Shown is the exchange coefficient $\overline{k_{ex}}$ in units of 10^{-2} mol m^{-2} yr^{-1} μatm^{-1}. The annual average map of the 12 monthly coefficient fields is shown in Figure 8. These maps basically reflect the spatial structure of the windfields (see Figure 4), however, the non-linearity of the LM-parametrization considerably enhances the contrasts in the coefficient fields between regions of weak and regions

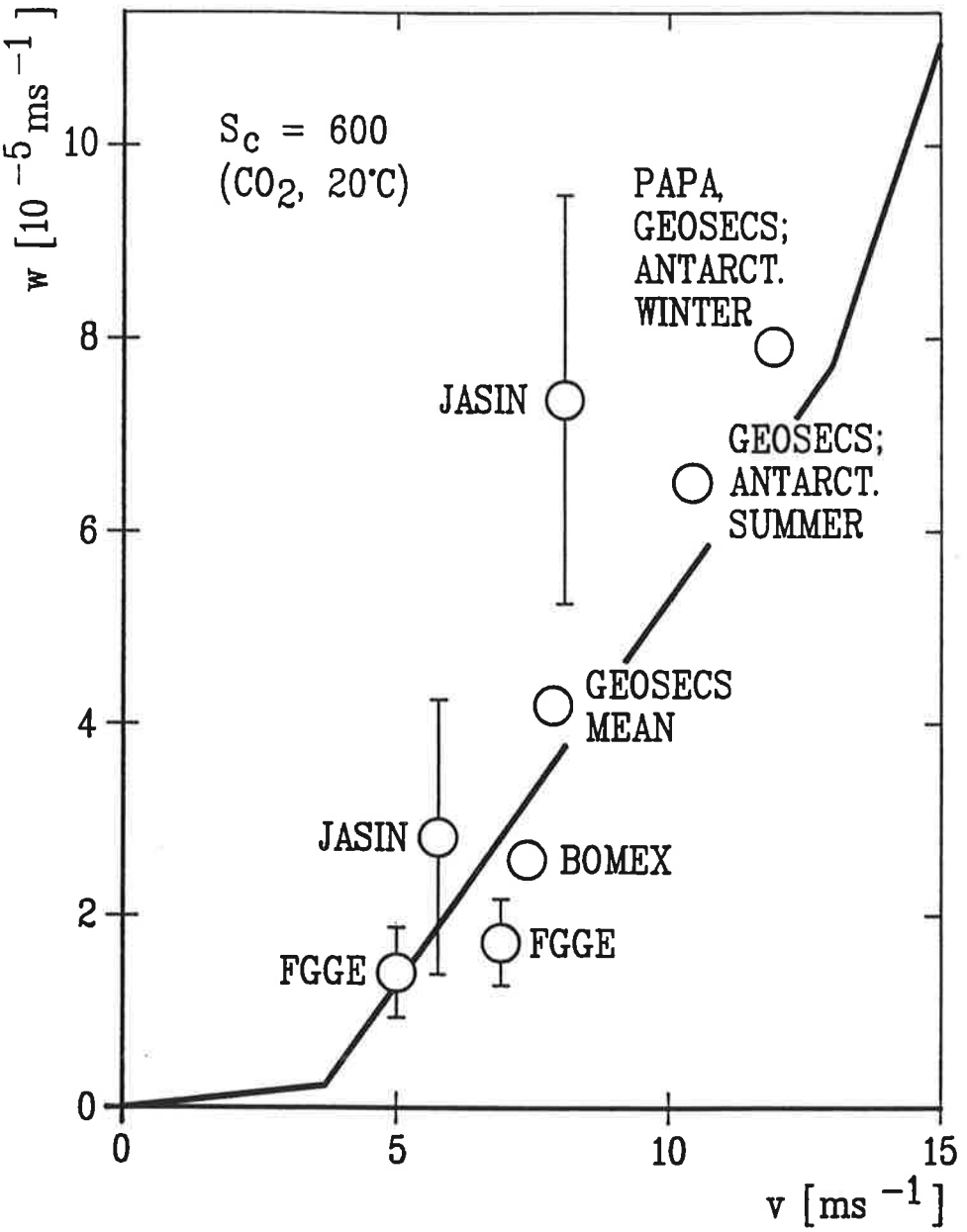

Figure 6: Piston velocity as function of windspeed for a gas with a Schmitt number of 600. Solid line: LM-parametrization (equation (5), Liss and Merlivat, [1986]). Symbols denote field measurements normalized to a Schmitt number of 600 obtained with the Radon method as summarized by Roether [1986].

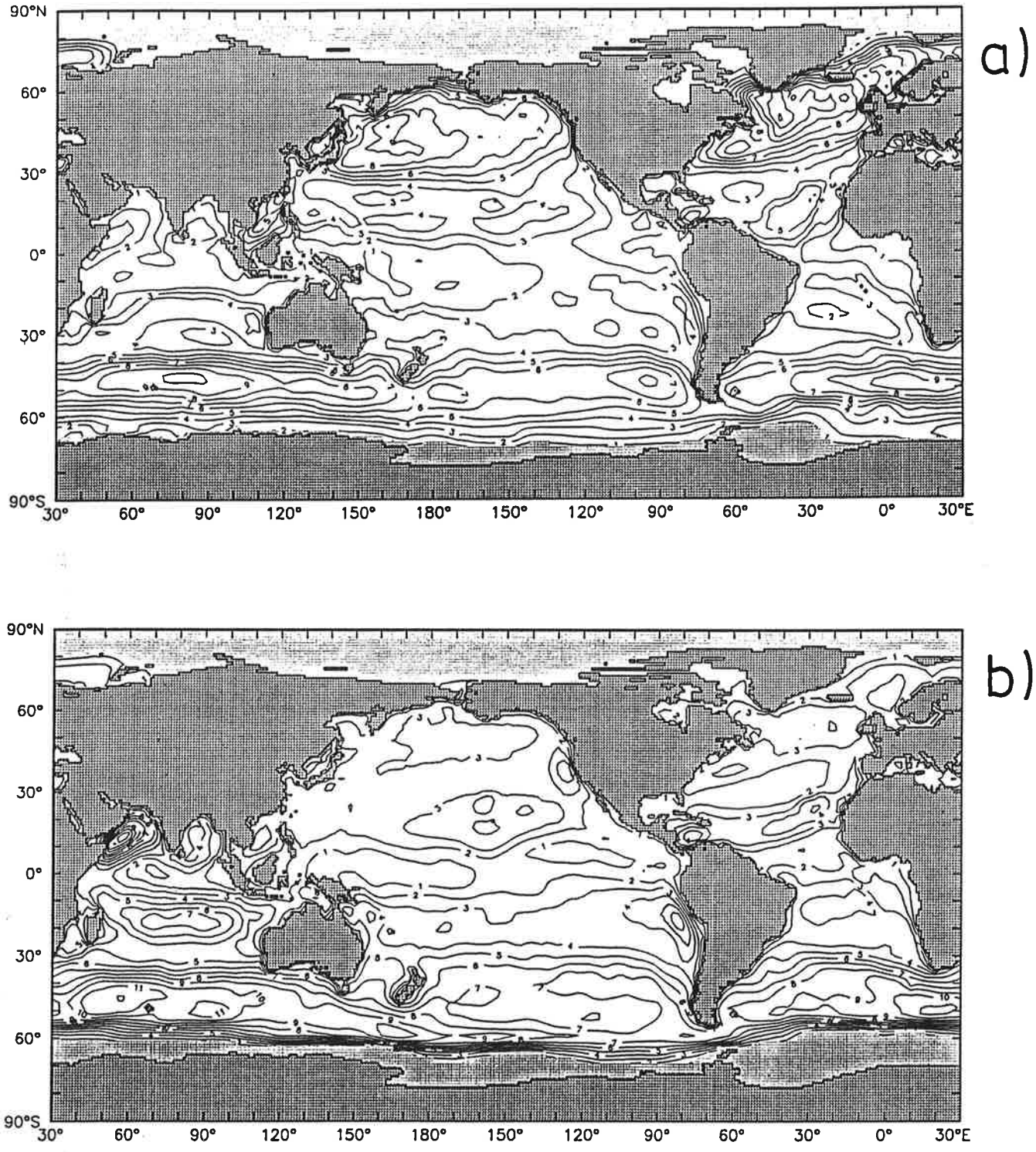

Figure 7: Map of the gas exchange coefficient for CO_2, k_{ex}, for (a) January and (b) July. Contour interval is 10^{-2} mol m^{-2} yr^{-1} μatm^{-1}. Stippled areas over the ocean represent ice-cover of more than 80%.

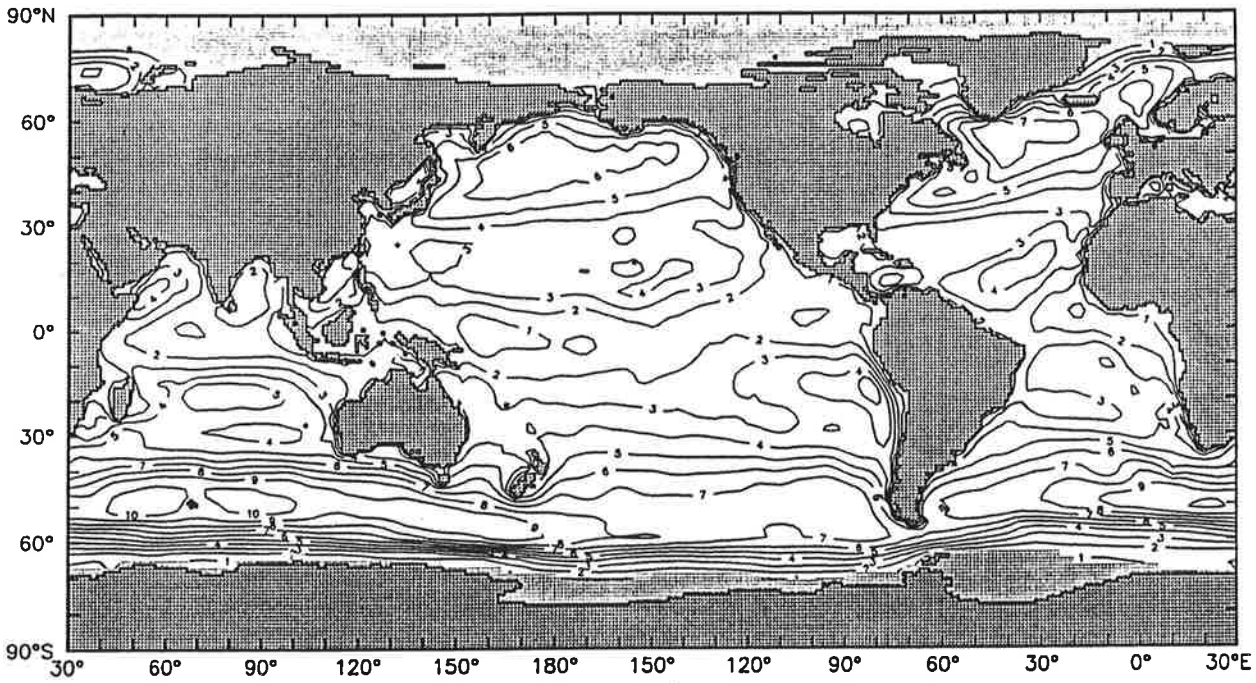

Figure 8: Same as Figure 7 but for the annual average.

of strong windspeeds. For example in July the highest mean windspeeds are found in the southern Indian Ocean, reaching values of 13 ms^{-1} whereas the lowest windspeeds found in the western equatorial Pacific lie around 3 ms^{-1}. On the map of the exchange coefficient for July the values in the same regions are 0.11 mol m^{-2} yr^{-1} $\mu atm^{-1}$and 0.01 mol m^{-2} yr^{-1} μatm^{-1}, respectively.

The highest values of the gas exchange coefficient in the southern hemisphere (0.11 mol m^{-2} yr^{-1} μatm^{-1}) are located in the Indian Ocean at a latitude of 50°S. In the northern hemisphere maximal values are found in the North Pacific (0.06 mol m^{-2} yr^{-1} μatm^{-1}) and in the North Atlantic (0.07 mol m^{-2} yr^{-1} μatm^{-1}). The lowest exchange coefficients (0.01–0.02 mol m^{-2} yr^{-1} μatm^{-1}) are found in the equatorial zone between 10°S and 10°N.

Figure 9 shows the zonally averaged exchange coefficient as function of latitude and time of the year. The seasonal variation is most pronounced in the northern hemisphere, values in winter being twice as large as in summer. In the southern hemisphere the seasonal cycle is less marked. Here the belt with maximal exchange coefficients shows a latitudinal shift of about 10° between summer and winter. A similar annual latitudinal shift is displayed by the region of minimal values in the Tropics.

Table 4 lists the numerical values of the zonally and annually averaged gas exchange coefficient for CO_2 as a function of latitude for each of the three major oceans and also for the entire ocean surface. In each ocean the coefficient displays a similar latitudinal structure. However, we find some quantitative differences, most notably in the Indian Ocean, which, at 45°S, exhibits a coefficient almost 20% higher than in the other two oceans. This incident significantly influences the regional repartitioning of the input of natural and bomb produced radiocarbon to the ocean [Monfray et al., 1989].

Approximate annually averaged coefficients for gases with Schmitt number and solubility dif-

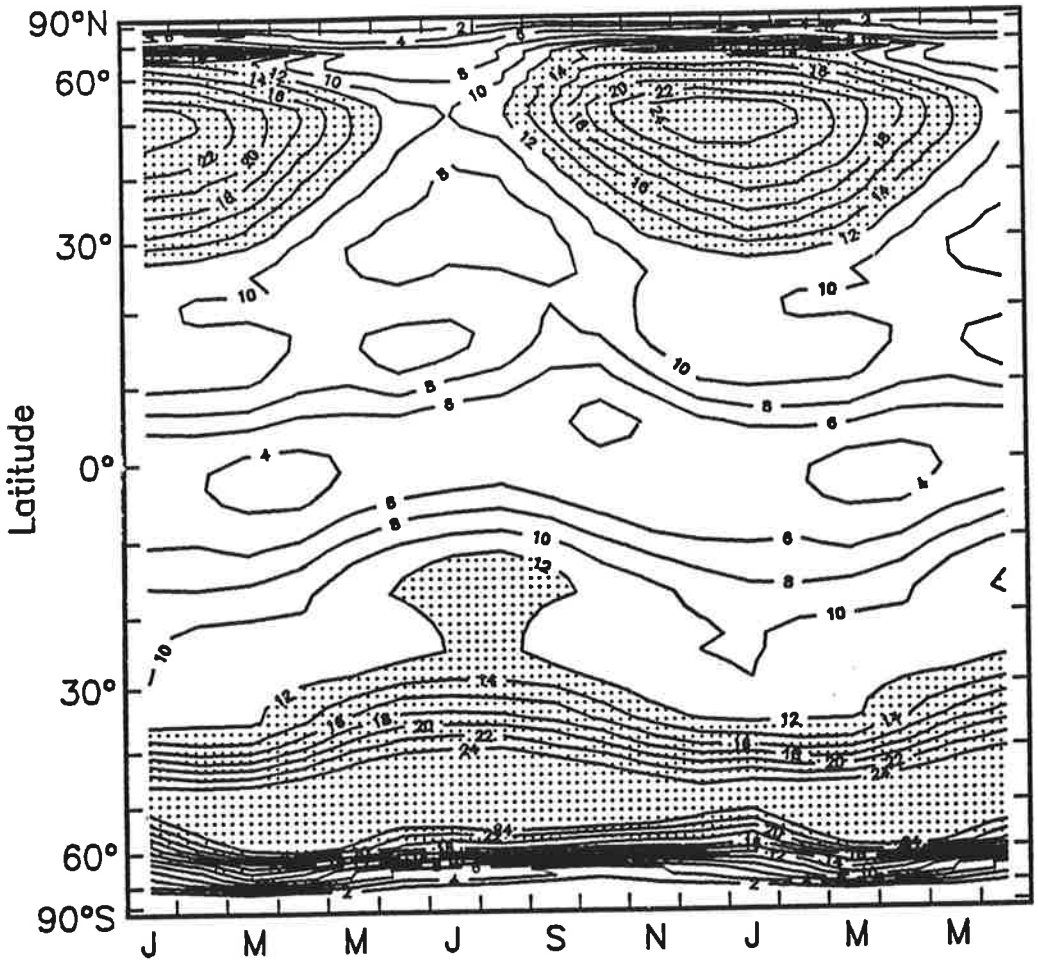

Figure 9: Zonally averaged gas exchange coefficient displayed versus time of the year. The first 6 months are shown twice to indicate the seasonality more clearly. Contour interval is 10^{-2} mol m^{-2} yr^{-1} μatm^{-1}. Stippled areas indicate values above 4 10^{-2} mol m^{-2} yr^{-1} μatm^{-1}.

Table 4: Zonal Annual Mean Gasexchange Coefficient for CO_2 [10^{-2}mol m^{-2} yr^{-1} μatm^{-1}]

Latitude	Atlantic	Pacific	Indian	Global Ocean
85°N	0.05			0.05
75°N	1.11			1.04
65°N	3.89	3.06		3.47
55°N	5.83	4.97		5.14
45°N	4.88	5.46		5.04
35°N	3.54	4.35		3.89
25°N	2.74	3.28	1.84	2.95
15°N	3.33	3.04	2.53	2.97
5°N	1.96	1.65	2.02	1.74
5°S	2.47	1.57	1.73	1.73
15°S	3.17	2.87	3.42	3.08
25°S	3.32	3.36	4.04	3.51
35°S	5.19	4.44	5.31	4.86
45°S	7.68	6.52	8.92	7.66
55°S	6.02	7.83	7.98	7.41
65°S	1.32	4.04	2.30	2.82
75°S	0.05	0.42		0.30

ferent than CO_2 may be derived from the values listed in Table 4 and the corresponding sea surface temperatures (Table 5), as explained in Appendix C.

4 Discussion

The derived gas exchange coefficient fields may be validated by basically two methods: Firstly, we could compare our results with direct measurements obtained by means of an analog trace gas, such as e.g. ^{222}Rn. However, at no place are the available data reliable enough to establish a climatologically significant monthly mean. Indeed, a pointwise comparison of a preliminary version of our coefficients with GEOSECS and TTO data [Peng et al., 1979, Smethie et al., 1985] revealed considerable scatter.
Alternatively, we may explore the global implications of our coefficient fields in the light of previous carbon cycle studies. Three principal global features warrant a validation:

1. The global annual mean of the coefficient fields;
2. The contrast of the mean annual field between high and low latitudes;
3. The seasonal cycle of the coefficient in temperate and high latitudes (primarily in the northern hemisphere).

Here we shall test items (1) and (2) by consideration of the observed distribution of the carbon isotopes ^{13}C and ^{14}C in the atmosphere and the ocean. We are not aware of a similar global test to adress item (3).

4.1 The global annual mean exchange coefficient

The annual average of the gas exchange coefficient over the entire ocean surface calculated from the fields as described in the previous section results in 0.0356 mol m^{-2} yr^{-1} μatm^{-1}. At

Table 5: Zonal Annual Mean Sea Surface Temperature [°C]

Latitude	Atlantic	Pacific	Indian	Global Ocean
85°N	0.0			0.0
75°N	0.9			0.9
65°N	4.9	3.2		4.5
55°N	8.3	5.9		7.0
45°N	13.0	9.9		11.1
35°N	20.7	18.6		19.4
25°N	24.5	23.9	26.8	24.2
15°N	26.1	27.0	27.7	26.9
5°N	27.2	27.7	28.2	27.7
5°S	26.0	26.9	28.0	27.0
15°S	24.0	25.8	26.7	25.7
25°S	22.1	22.7	23.1	22.6
35°S	17.6	17.6	17.5	17.5
45°S	8.9	11.4	9.2	10.0
55°S	1.7	5.7	2.0	3.4
65°S	0.1	0.8	0.3	0.4
75°S	0.0	0.0		0.0

an atmospheric partial CO_2 pressure of 330 μatm, this value corresponds to an average CO_2 exchange rate of 11.7 mol m^{-2} yr^{-1}. Using an atmospheric carbon content of 5.10 10^{16} moles at an atmospheric partial CO_2 pressure of 290 μatm and an ocean surface area of 3.62 10^{14} m^2, we obtain a residence time of 13.6 years for atmospheric CO_2 gas with respect to exchange with the ocean.

This average value is a factor of 1.7 lower than estimates based on either the natural radiocarbon balance or on the estimated uptake of bomb-produced radiocarbon by the oceans which result in 0.061±0.010 mol m^{-2} yr^{-1} μatm^{-1} [Broecker et al., 1986]. A more detailed analysis of the radiocarbon estimates, which takes into account the spatial covariance between exchange coefficient as calculated from the LM-parametrization and the atmospheric and oceanic ^{14}C data, but also local imbalances of the net CO_2 air-sea flux, reduces the discrepancy to a factor of 1.6. Only less than 50% of this discrepancy can be explained by uncertainties in the available ^{14}C data [Monfray et al., 1989].

As there is no obvious reason to question the radiocarbon estimates we have to investigate the validity of our analysis of surface windspeed data. Two sources of error could lead to an underestimate of the final result: Either the monthly mean values are too low due to some bias in the assimilation scheme of the ECMWF, or the estimated standard deviations of the instantaneous windspeed are too small due to the inevitable spatial smoothing involved in the data analysis.

By increasing windspeed and standard deviations in equation (7) we find that a global factor of 1.3 is needed in order to increase the global mean exchange coefficient to the radiocarbon data based value. Our pointwise checks of the analyses with high quality weathership and buoy data did reveal systematic discrepancies exceeding 25% only at two of the tropical locations. Furthermore, the differences between archived ship reports and meteorological analyses were found to be small (see Section 2, and in particular Figure 2). It is therefore quite unlikely that our windspeed estimates be a global factor of 1.3 smaller than the real values.

Increasing the standard deviation of windspeed would also enhance the global mean exchange

coefficient because of the non-linearity of the LM-parametrization. However, the sensitivity of the calculation with respect to this feature is rather small: if we amplify the standard deviations globally by a factor of 1.5 the global mean exchange coefficient increases only by a factor of 1.13. In view of the results presented in Section 2 it is impossible that we have underestimated the true windspeed dispersion by a factor of 2 or more.
Finally, Etcheto and Merlivat [1988] find in their study a global average exchange coefficient of 0.036 mol m^{-2} yr^{-1} μatm^{-1}. Their estimate is based on the same LM-parametrization formula as used in the present study, but they employed independent windspeed data, derived from scatterometer data of the Seasat satellite, which was in operation during the period July to September 1978. The result of Etcheto and Merlivat [1988] is very close to the mean value as calculated in the present study. We also find that the global average derived from only the 3 months does not show any significant bias with respect to the annual global average: if we compute the average only for the time period July to September we obtain 0.0358 mol m^{-2} yr^{-1} μatm^{-1}, which is less than 1% larger than the annual average.
Thus we conclude that the discrepancy between the global mean exchange coefficient as calculated above and the estimate based on radiocarbon data may not be explained by systematic errors in the windspeed data. It appears more likely that the relationship proposed by Liss and Merlivat [1986] needs some modification, especially regarding the fact that it has been derived from a single lake experiment which might not be representative for all conceivable open ocean conditions. In particular, at a given windspeed one could expect quite different wave spectra over the sea than over a lake. In view of these limitations it is quite surprising that the LM-parametrization formula in conjunction with available ocean windspeed statistics results in a global average which is consistent with the existing ^{14}C data within a factor of 1.6.
For global carbon cycle modelling studies it is of course an advantage to use an exchange coefficient for CO_2 which conforms to the ^{14}C data. To this end we can think of three kind of *ad hoc* adjustments to the presently established fields:

1. The relation postulated by LM could be multiplied by a factor of 1.6.

2. The regime of breaking waves, which is believed to enhance gas transfer due to the effect of bubbles, [Merlivat and Memery, 1983] is not well known. We note, however, that the last term in equation (5) would have to be increased by a factor of more than 16 in order to increase the global average coefficient by the required factor of 1.6.

3. The relation (5) could be contracted linearly in the v_{10}-direction by a factor of 1.3 (equivalent to a global increase of the windspeed estimates by a factor of 1.3).

In the accompanying article [Monfray et al., 1989] we choose to calibrate all coefficient fields by a uniform factor of 1.6.

4.2 The contrast between low and high latitudes

The most striking feature in Figures 7 and 8 is the strong contrast of the magnitude of the gas exchange coefficient between high and low latitudes which exceeds a factor of 4. If it is real it would have serious implications on the oceanic uptake and redistribution of bomb radiocarbon, as noted by Broecker et al., [1985] and explored in depth in the accompanying article [Monfray et al., 1989]. This contrast reflects the variations in the windspeed fields which are emphasized because of the non-linearity of the LM-parametrization. If the piston velocity were simply a linear function of windspeed the ratio between the values in high and low latitudes would be reduced to 2.5.
This feature of the gas exchange coefficient fields may be validated (at least in principle) by the preindustrial, assumed steady state distribution of the stable carbon isotope ratio $^{13}C/^{12}C$ in

atmospheric CO_2 and in dissolved inorganic carbon in the surface ocean. The heavier ^{13}C isotope is fractionated relative to the ^{12}C isotope at the air-sea interface, the degree of fractionation being a well known function of temperature. Hence, in a steady state, the mean air-sea difference of the $^{13}C/^{12}C$ ratio essentially should reflect the mean sea surface temperature weighted by the CO_2 gas exchange coefficient.
More precisely, assuming a steady state, we require that the globally averaged air-sea flux of ^{13}C, $< {}^{13}F >$, vanishes:

$$< {}^{13}F > = < R_a F_{am} \alpha'_{am} > - < R_m F_{ma} \alpha'_{ma} > = 0 \tag{8}$$

where R_a and R_m denote the $^{13}C/(^{13}C+^{12}C)$ ratio in the atmosphere and in the surface ocean, respectively; F_{am} represents the gross flux of CO_2 into and F_{ma} the gross flux out of the water. α'_{am} and α'_{ma} are the kinetic fractionation factors (see e.g. Siegenthaler and Münnich [1981]). The symbol $< x >$ denotes the annual and global average of the quantity x.
Equation (8) may be reexpressed as follows:

$$< r_a k_{ex} P_a \alpha_{am} > = < r_m k_{ex} P_m \alpha_{ma} > \tag{9}$$

Here we have approximated the $^{13}C/(^{13}C+^{12}C)$ ratios, R_a and R_m, by their corresponding $^{13}C/^{12}C$ ratios, r_a and r_m. Correspondingly, the α_{am} and α_{ma} in equation (9) refer to the kinetic fractionation factors for the $^{13}C/^{12}C$ ratios. Both fractionation factors are known functions of the absolute temperature, T, [Mook, 1986] which may be expressed as

$$\alpha_{am} = 1 + \epsilon_{am} = 1 + c_1 + d_1 T^{-1} \tag{10}$$

and

$$\alpha_{ma} = 1 + \epsilon_{ma} = 1 + c_2 + d_2 T^{-1} \tag{11}$$

The numerical values of the constants c_1, d_1, c_2, d_2 are listed in Appendix D.
Furthermore, we reexpress P_m as

$$P_m = P_a(1 + \pi_m) \tag{12}$$

At most places over the ocean the partial pressure of CO_2 in surface waters is close to the atmospheric value, hence in general $|\pi_m| \leq 0.1$.
Inserting (10), (11) and (12) into (9) we obtain

$$< r_a P_a (1 + \epsilon_{am}) k_{ex} > = < r_m P_a (1 + \pi_m)(1 + \epsilon_{ma}) k_{ex} > \tag{13}$$

This equation may be approximated by

$$< r_a >< P_a > (< k_{ex} > + < \epsilon_{am} k_{ex} >) = < r_m >< P_a > (< k_{ex} > + < \pi_m k_{ex} > + < \epsilon_{ma} k_{ex} >) \tag{14}$$

The simplification on the left hand side of (14) is justified because the atmospheric partial pressure of CO_2, P_a, and the atmospheric $^{13}C/^{12}C$ ratio, r_a, are spatially almost constant and do not covary with k_{ex} nor ϵ_{am}. The same argument is used on the right hand side, although existing data on $< r_m >$ might not be sufficient to strictly prove this assertion (see below). Furthermore we have neglected the term involving the product of π_m and ϵ_{ma}. Moreover, assuming a steady state not only with respect to ^{13}C but also with respect to CO_2 requires

$$< \pi_m k_{ex} > = 0 \tag{15}$$

Simplifying equation (14) and using (10) and (11) we obtain

$$< r_a > = < r_m > \frac{1 + c_2 + d_2 \frac{< k_{ex} T^{-1} >}{< k_{ex} >}}{1 + c_1 + d_1 \frac{< k_{ex} T^{-1} >}{< k_{ex} >}} \tag{16}$$

$$= < r_m > \frac{1 + c_2 + d_2 T_{eff}^{-1}}{1 + c_1 + d_1 T_{eff}^{-1}} \tag{17}$$

The steady state air-sea partitioning of the $^{13}C/^{12}C$ isotope ratio is thus seen to depend primarily on an effective sea surface temperature, T_{eff}, which is determined from a weighted average of the actual sea surface temperatures

$$T_{eff}^{-1} = \frac{< k_{ex} T^{-1} >}{< k_{ex} >} \tag{18}$$

Based on the gas exchange coefficient fields calculated from the LM-parametrization we obtain

$$T_{eff} = 15.06°C \tag{19}$$

This value is lower than the global average sea surface temperature of 19.13°C as calculated from the Levitus data set, since the k_{ex}-fields give more weight to temperate and high latitude regions. From the numerical values of the fractionation factors (Appendix D) we find that in a steady state the atmospheric $^{13}C/^{12}C$ ratio should be 8.97‰ lower than the corresponding average $^{13}C/^{12}C$ ratio of dissolved inorganic carbon in the surface ocean.
The sensitivity of the present calculation is illustrated by performing the same calculation as above but using a spatially and temporally uniform exchange coefficient. In this case the equilibrium air-sea fractionation results in only 8.51‰, obtained from an effective sea surface temperature of 19.13°C. Likewise, if the gasexchange coefficient were assumed to be simply proportional to windspeed, we find an effective temperature of 17.59°C corresponding to an air-sea fractionation of 8.68‰.
Therefore, given accurate preindustrial atmospheric and surface ocean $^{13}C/^{12}C$ ratios it should be possible to verify the theoretical fractionation as calculated above. An accuracy of better than 0.2‰, however, is required to effectively distinguish between the two extreme predictions above (uniform gas exchange coefficient against LM-parametrization). This is well above the measurement precision which currently can be achieved, though possible systematic biases are discussed below. What were the preindustrial $^{13}C/^{12}C$ ratios in the atmosphere and in the surface ocean?
Friedli et al. [1986] have measured the $^{13}C/^{12}C$ on CO_2 extracted from air-bubbles enclosed in Antarctic ice. They report a value of -6.44 ± 0.15‰. (We use the common notation of expressing $^{13}C/^{12}C$ ratios by the reduced ratio, δ, which is defined as $\delta = r/r_s - 1$, where r_s denotes the $^{13}C/^{12}C$ ratio of the PDB standard.)
Figure 10 displays measurements of the $^{13}C/^{12}C$ ratio on dissolved inorganic carbon in the surface ocean as a function of latitude, obtained by Kroopnik during the GEOSECS program [Kroopnik, 1985] between 1971 and 1978. The data show considerable scatter, but no clear latitudinal structure is discernible. The mean of all 135 datapoints is 1.70‰ and the standard deviation results in 0.32‰. These data, however, are not directly representative of the preindustrial surface ocean $^{13}C/^{12}C$ ratios values since they have been negatively perturbed due to the anthropogenic fossil fuel CO_2 (the so-called ^{13}C-Suess effect). Coral ^{13}C-data [Nozaki et al., 1978, Druffel and Benavides, 1986] but also global carbon cycle model calculations [Siegenthaler and Oeschger, 1987] show this effect in the surface ocean layer to amount to -0.4 to -0.5‰.
The observations thus suggest a preindustrial air-sea fractionation of 8.59‰ with a statistical error of perhaps 0.16‰ (one standard deviation). If this value is compared to the theoretical prediction as calculated above using the exchange coefficient based on the LM-parametrization we notice a difference of 0.4‰. Is this remaining difference of 0.4‰ significant, i.e. does it indicate, that the calculated strong contrast between low and high latitudes of the exchange coefficient for CO_2 has to be ruled out because of the preindustrial ^{13}C-equilibrium argument? Several effects might bias the present calculation:

1. Seasonal bias of surface ocean $^{13}C/^{12}C$ data. GEOSECS data were obtained exclusively in summer and hence might not be representative of the annual average. We are not aware

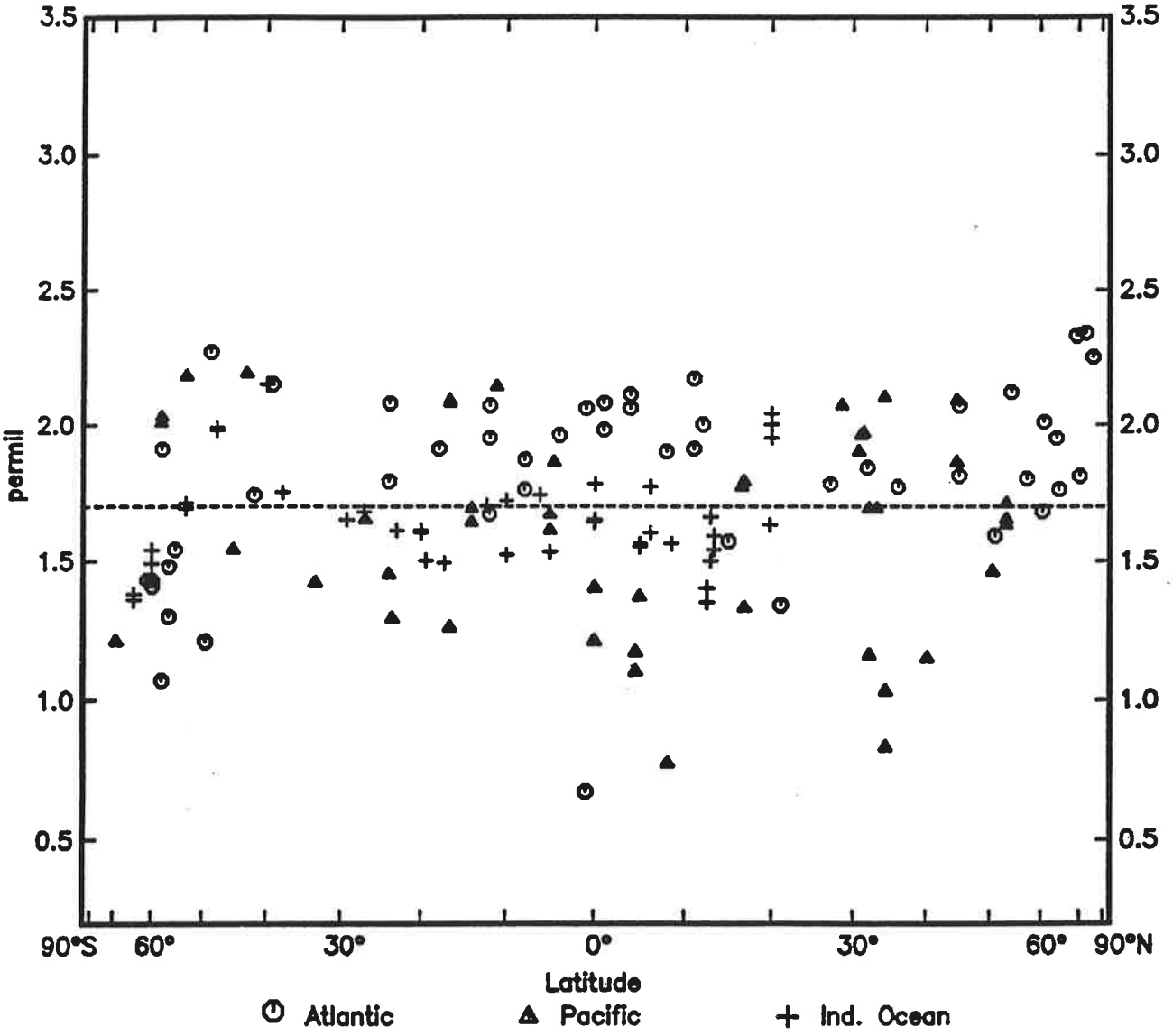

Figure 10: $^{13}C/^{12}C$ ratio of dissolved inorganic carbon in the surface ocean as a function of latitude [Kroopnik, 1985]. The symbols indicate individual oceans; circles: Atlantic, triangles: Pacific, crosses: Indian ocean. The dashed line indicates the global average.

of any measurements of the seasonal cycle of ^{13}C in surface waters. We note however, that both, mixing in winter with subsurface waters and increased biological productivity in summer would lead to higher δ values of dissolved inorganic carbon in summer as compared to winter. Hence the annual average would still be lower than Kroopnik's data and result in a smaller observed air-sea fractionation; in contrast to the theoretical prediction.

2. Representativity of GEOSECS data. It is very difficult to assess the representativity of the existing $^{13}C/^{12}C$ data of dissolved inorganic carbon in surface ocean waters. Indeed, we try to estimate the global average from mere 135 datapoints! Nevertheless, the GEOSECS program covered all major oceans. Examination of Kroopnik's surface ocean ^{13}C data as a function of location did not reveal any clear spatial structures, hence we attribute the scatter in the data (see Figure 10) to local inhomogenities and to the measurement precision.

3. Biased preindustrial atmospheric ^{13}C value. The ice core measurements of Friedli et al. [1986] are the only available preindustrial atmospheric ^{13}C data todate. Recently, Schwander [1989] and Craig et al. [1988] have discussed the effects of gravity separating gases and isotopes in the firn layer above the solid ice. Because of this effect the possibility exists that the the ^{13}C data of Friedli et al. [1986] reflect values which are more positive (i.e. ^{13}C enriched) than the overlying atmosphere at the time when the air bubbles were trapped in the ice. For the Siple Station in West Antarctica, where the ^{13}C data have been obtained the magnitude of this effect is predicted to be at most 0.3 to 0.4 ‰. If the gravity effect is really that large the observed preindustrial air-sea fractionation would be increased to 8.9‰ and thus confirm the theoretical prediction based on the LM-parametrization of the gas exchange coefficient.

4. Preindustrial steady state. The assumption of a preindustrial steady state in the carbon system might be challenged. Although Siegenthaler et al. [1988] find excursions in the atmospheric ^{13}C record as determined from ice cores, these variations do not exceed 0.2‰.

5. Calibration Problems. Since we are comparing ^{13}C data from two different laboratories there exists the possibility of systematic offsets due to calibration problems. ^{13}C measurements from other laboratories could help to rule out calibration problems. We are aware of only one other published sea surface ^{13}C data set from a limited area in the western Pacific ocean [Inoue et al., 1987]. These data exhibit a mean of 1.56±0.31‰ which is close to the data reported by Kroopnik [1985].

6. Suess effect. Is it possible that we underestimate the size of the surface ocean Suess effect? We hesitate to accept this possibility, since it would imply serious consequences with respect to carbon cycle modelling.

Given the aforementioned uncertainties it is not possible to establish the preindustrial ^{13}C air-sea equilibrium fractionation with the required precision in order to distinguish between the different theoretical sensitivity predictions presented above. If the ice core data have to be corrected because of the gravity effect then the observations would be consistent with the LM-parametrization of the gas exchange coefficient; but even without this correction, pending further sea surface ^{13}C data with the required precision and temporal and spatial coverage we must conclude, that the high-low latitude contrast in the coefficient fields based on the LM-parametrization cannot be confirmed or ruled out by the present argument.

5 Conclusions

Using archived ship reports and meteorological analyses we have constructed a global, monthly climatology of mean and standard deviation of surface windspeed over the ocean. Assuming a Weibull frequency distribution of the surface windspeed we evaluated the gas exchange coefficient for CO_2 based on the relationship proposed by Liss and Merlivat [1986]. Two aspects of the final product have been investigated through analysis of carbon isotope data: the global mean value of the exchange coefficient and the contrast between high and low latitudes. The global mean value is found a factor of 1.6 too small in order to be compatible with the existing oceanic ^{14}C data. Due to uncertainties in the available ^{13}C data the contrast between high and low latitudes in the predicted coefficient fields cannot yet be tested conclusively.

We find a fair agreement between surface windspeed data from direct observations, archived ship reports and meteorological analyses, but also from satellite data as implied by the results of Etcheto and Merlivat [1988]. Based on this consideration an improvement of the present estimates of the gas exchange coefficient, on a global scale, depends not primarily on better surface windspeed estimates, but has to await a more comprehensive microphysical model of the gas exchange process, supplemented with direct open ocean measurements.

Nevertheless, the present product may be of use in modelling studies of the uptake and redistribution of CO_2 and ^{14}C in the ocean [Monfray et al., 1989]. Similarly, the constructed fields of the gas exchange coefficient may be applied with few modifications to other low to moderately soluble gases of interest beside CO_2, such as e.g. ^{222}Rn, DMS, and light hydrocarbons. The datasets compiled in the present study (monthly fields of windspeed, standard deviation, temperature, ice-cover and gas exchange coefficient on a 2° by 2° grid) on magnetic tape may be requested from the authors.

A Analytical reexpression of integral (7) in terms of incomplete gamma functions

Integral (7) can be solved exactly since $w(v)$ may be written as a sum

$$w(v) = \sum_{i=1}^{3} w_i(v) = \sum_{i=1}^{3} A_i(v - v_i)\,\mathrm{U}(v - v_i) \tag{20}$$

(see equation (5)).
Integral (7) is therefore also given by a sum:

$$\overline{w} = \sum_{i=1}^{3} W_i \tag{21}$$

where each of the terms W_i is given by

$$W_i = \int_0^\infty f(v) w_i(v) dv = A_i \int_{v_i}^\infty (v - v_i) \frac{a}{c} e^{-(\frac{v}{c})^a} (\frac{v}{c})^{a-1}\, dv \tag{22}$$

which may be reexpressed as

$$W_i = A_i \left\{ c\, Q(\frac{1}{a} + 1, (\frac{v_i}{c})^a) - v_i e^{-(\frac{v_i}{c})^a} \right\} \tag{23}$$

The incomplete Γ-function, $Q(b, x)$, is defined as

$$Q(b, x) = \int_x^\infty e^{-t} t^{b-1}\, dt \tag{24}$$

[Abramowitz and Segun, p. 260, 1965].

B Schmitt number and solubility of CO_2

The Schmitt number, Sc, was specified as a function of absolute temperature, T, according to

$$Sc = 10^{-3.889 + 1955\, T^{-1}} \tag{25}$$

which was obtained by fitting a function of the form $A + BT^{-1}$ to the logarithm of the Schmitt number data for CO_2 reported by Jähne et al. [1987].
The solubility of the CO_2 gas was specified using the formula given by Weiss [1974], where α_s is expressed in mol l^{-1} atm^{-1}:

$$\begin{aligned} \ln(\alpha_s) \;=\; & -58.0931 + 9050.69/T + 22.2940 \ln(T/100) \\ & + S(0.027766 - 0.025888(T/100) + 0.0050578(T/100)^2) \end{aligned} \tag{26}$$

where S denotes the salinity expressed in ‰.

C Exchange coefficient for gases other than CO_2

The data presented in Table 4 may be used to obtain estimates of the exchange coefficient, k'_{ex}, for a gas other than CO_2 by means of

$$k'_{ex} \approx k_{ex}(\mathrm{CO_2}) \frac{\alpha_s(T)'}{\alpha_s(T, \mathrm{CO_2})} \left[\frac{Sc(T)'}{Sc(T, \mathrm{CO_2})} \right]^{-\frac{1}{2}} \tag{27}$$

where primed quantities refer to the other gas under consideration. Equation (27) is not exact since it assumes throughout the entire domain of windspeeds a $(-\frac{1}{2})$-power law for the dependency of the piston velocity on the Schmitt number, contrary to the LM-parametrization (5). Furthermore, if equation (27) is used to estimate annual mean exchange coefficients from the numbers listed in Tables 4 and 5, the covariance between temperature and piston velocity within each latitude band and during the annual cycle is neglected.

D Temperature dependence of the kinetic fractionation factors

The kinetic fractionation factor, α_{ma}, is the product of the equilibrium fractionation factor, α_{DIC}, of dissolved CO_2 with respect to total dissolved inorganic carbon, multiplied by the ratio of the transfer velocities of $^{13}CO_2$, w^*, and of CO_2, w:

$$\alpha_{ma} = \alpha_{DIC}\frac{w^*}{w} \tag{28}$$

The other kinetic fractionation factor, α_{am}, is the product of the equilibrium fractionation factor, α_β, of dissolved CO_2 with respect to gaseous CO_2, times the ratio of the transfer velocities w^* and w:

$$\alpha_{am} = \alpha_\beta\frac{w^*}{w} \tag{29}$$

No significant temperature dependence of the w^*/w ratio has been observed [Wanninkhof, 1985], here we assume it to be constant in space and time.
For the temperature dependence of the equilibrium fractionation factor α_β we use

$$\alpha_\beta = 1 + 0.00019 - 0.373\,T^{-1} \tag{30}$$

(Mook, 1986). T denotes the absolute temperature expressed in K.
The temperature dependence of α_{DIC} depends on the relative partitioning of total dissolved carbon into H_2CO_3, HCO_3^- and $CO_3^=$ [Mook, 1986]. We neglect the contribution by H_2CO_3 and assume a partitioning of 90% HCO_3^- and 10% $CO_3^=$. α_{DIC} is then given by

$$\alpha_{DIC} = 1 + 0.02387 - 9.779\,T^{-1} \tag{31}$$

Acknowledgments. We thank C.D. Keeling for several constructive discussions. We acknowledge the German Wetterdienst for providing the weathership data and the analyses of the ECMWF, which we accessed through routines kindly made available to us by the Meteorological Institute of the University of Hamburg. We thank M.J. McPhaden, C. Colin and J. Boutin for letting us inspect the surface windspeed data from the equatorial Pacific and Atlantic ocean buoys. We thank P. Wright for providing us the COADS data set and we appreciate the programming support by by C. Jahnke. P. M. was supported by the Commission of the European Communities' climatology and natural hazards program (contract no. EV4C-0030-D(B)).

E References

Abramowitz, M. and I. A. Segun *Handbook of mathematical functions,* Dover, New York, 1046pp., 1965.

Alexander,R.C. and R.L.Mobley, Monthly average sea surface temperatures and ice pack limits on a 1deg global grid, *Mon. Weather Rev., 104,* 143–148, 1976.

Bengtsson, L., M. Kanamitsu, P. Kallberg, and S. Uppala, FGGE 4-dimensional data assimilation at ECMWF, *Bull. Amer. Met. Soc., 69,* 29–43, 1982.

Black, D. D. and M. J. McCready, Effect of small-wavelength waves on gas transfer across the ocean surface, *J. Geophys. Res., 93,* 5143–5152, 1988.

Bolin B., C.D. Keeling, R.B. Bacastow, A. Björkström and U. Siegenthaler, Carbon cycle modelling, in: *SCOPE 16 Carbon cycle modelling,* edited by B.Bolin, Wiley, New York, 1–28, 1981.

Broecker, W. S., J. R. Ledwell, T. Takahashi, R. Weiss, L. Merlivat, L. Memery, T.-H. Peng, B. Jähne, and K. O. Münnich, Isotopic versus micrometeorologic ocean CO_2 fluxes: a serious conflict, *J. Geophys. Res., 91,* 10517–10527, 1986.

Broecker, W. W., T.-H. Peng, G. Östlund, and M. Stuiver, The distribution of bomb radiocarbon in the ocean, *J. Geophys. Res., 90,* 6953–6970, 1985.

Broecker, W. S. and T.-H. Peng, Tracers in the sea, Lamont-Doherty Geological Observatory, Columbia University, Palisades, New York, 690pp., 1982.

Coantic, M., A model of gas transfer across air-water interfaces with capillary waves, *J. Geophys. Res., 91,* 3925–3943, 1986.

Colin, C., and S. L. Garzoli, In situ wind measurements and the ocean response in the equatorial Atlantic during the Atlantic Ocean Experiment, *J. Geophys. Res., 92,* 3729–3740, 1987.

COADS, Comprehensive Ocean-Atmosphere Data Set, Release 1, NCAR, Boulder, Colorado, 1985.

de Boor C., A practical guide to splines, Springer, New York, 392pp., 1978.

Druffel, E. M. and L. M. Benavides, Input of excess CO_2 to the surface ocean based on $^{13}C/^{12}C$ ratios in a banded Jamaican sclerosponge, *Nature, 321,* 58–61, 1986.

Erickson, D. J., and R. A. Duce, On the global transfer velocity field of gases with a Schmidt number of 600, *Searex Newslett., 10,* 7–10, 1987.

Etcheto, J. and L. Merlivat, Satellite determination of the carbon dioxide exchange coefficient at the ocean-atmosphere interface: a first step, *J. Geophys. Res.,* in press, 1988.

Friedli, H., H. Lötscher, H. Oeschger, U. Siegenthaler and B. Stauffer, Ice core record of the $^{13}C/^{12}C$ ratio in the past two centuries, *Nature, 324,* 237-238, 1986.

Jähne, B., K.O. Münnich, R. Bösinger, A. Dutzi, W. Huber and P. Libner, On the parameters influencing air-water gas exchange, *J. Geophys. Res.,* Jan. 1987.

Jähne, B., G. Heinz, and W. Dietrich, Measurement of the diffusion coefficients of sparingly soluble gases in water, *J. Geophys. Res., 92,* 10767–10776, 1987.

Justus, C.G., W.R. Hargraves, A. Mikhail and D. Graber, Methods for estimating wind speed frequency distributions, *J. Appl. Meteorol., 17,* 350–353, 1978.

Kroopnik, P. M., The distribution of ^{13}C of ΣCO_2 in the world oceans, *Deep-Sea Res., 32,* 57–84, 1985.

Levitus, S., *Climatological atlas of the world ocean,* NOAA professional paper 13, Rockville, Md., 173pp., 1982.

Liss, P.S. and L. Merlivat, Air-sea gas exchange rates: Introduction and synthesis in: *The Role of Air-Sea Exchange in Geochemical Cycling,* P. Buat-Ménard Ed., Reidel, Dordrecht, 113–127, 1986.

Lorenc, A. C., A global three-dimensional multivariate statistical interpolation scheme, *Mon. Wea. Rev., 199*, 701–721, 1981.

Maier-Reimer, E. und K. Hasselmann, Transport and storage of CO_2 in the ocean – an inorganic ocean-circulation carbon cycle model, *Climate Dynamics, 2,* 63–90, 1987.

Monfray, P., Echanges océan/atmosphère du gaz carbonique: Variabilité avec l'état de la mer, Thesis, Université de Picardie, 258pp., 1987.

Monfray, P., Heimann, M. and E. Maier-Reimer, Spatial and temporal variation of the gas-exchange coefficient for CO_2: 2. Implications on the ^{14}C and CO_2 uptake by the oceans, in preparation, 1989.

Mook, W. G., ^{13}C in atmospheric CO_2, *Netherlands Journal of Sea Res., 20,* 211–223, 1986.

Nozaki, Y., D. M. Rye, K. K. Turekian, and R. E. Dodge, A 200 year record of carbon-13 and carbon-14 variations in a Bermuda coral, *Geophys. Res. Lett., 5,* 825–828, 1978.

Peng, T.-H., W. S. Broecker, G. G. Mathieu and Y.-H. Li, Radon evasion rates in the Atlantic and Pacific oceans as determined during GEOSECS program, *J. Geophys. Res., 84,* 2471–2486, 1979.

Roether W. and B. Kromer, Optimum application of the radon deficit method to obtain air-sea gas exchange rates, in *Gas Transfer at Water Surfaces,* edited by W. Brutsaert and G. H. Jirka, 447–457, Reidel, Dordrecht, 1984.

Roether, W., Field measurements of gas exchange, in: *Dynamic processes in the chemistry of the upper ocean,* Burton, J.D., Brewer, P.G. and R. Chesselet, (Eds.), Plenum Press, New York, 117–128, 1986.

Siegenthaler, U. and K. O. Münnich, $^{13}C/^{12}C$ fractionation during CO_2 transfer from air to sea, in SCOPE 16: *Carbon Cycle Modelling* (ed. B. Bolin), John Wiley and Sons, Chichester, 249-258, 1981.

Siegenthaler, U. and H. Oeschger, Biospheric CO_2 emissions during the past 200 years reconstructed by deconvolution of ice core data, *Tellus, 39B,* 140–154, 1987.

Smethie, W. M., T. Takahashi, D. W. Chipman, and J. R. Ledwell, Gas exchange and CO_2 flux in the tropical Atlantic ocean determined from ^{222}Rn and pCO_2 measurements, *J. Geophys. Res., 90,* 7005–7022, 1985.

Stewart, D.A. and O.M. Essenwanger, Frequency distribution of wind speed near the surface, *J. Appl. Meteorol., 17,* 1633–1642, 1978.

Thomas, F., C. Perigaud, L. Merlivat, and J. F. Minster, World scale monthly mapping of the CO_2 ocean-atmosphere gas transfer coefficient, *Phil. Trans. R. Soc.,* in press, 1988.

Wanninkhof, R., Kinetic fractionation of the carbon isotopes ^{13}C and ^{12}C during transfer of CO_2 from air to seawater, *Tellus, 37B,* 128–135, 1985.

Wanninkhof, R., J. R. Ledwell, and W. S. Broecker, Gas exchange-wind speed relation measured with sulfur hexafluoride on a lake, *Science, 227,* 1224–1226, 1985.

Weiss, R.F., Carbon dioxide in water and seawater; the solubility of a non-ideal gas, *Mar. Chem., 2,* 203–215, 1974.

Woodruff, S. D., R. J. Slutz, R. L. Jenne and P. M. Steurer, A Comprehensive Ocean-Atmosphere Data Set, *Bull. Amer. Met. Soc., 68,* 1239-1250, 1987.